Available online at www.sciencedirect.com

ScienceDirect

Procedia Manufacturing 51 (2020) 671–677

Procedia MANUFACTURING

www.elsevier.com/locate/procedia

30th International Conference on Flexible Automation and Intelligent Manufacturing (FAIM2021)
15-18 June 2021, Athens, Greece.

Direct Energy Deposition: a complete workflow for the additive manufacturing of complex shape parts

Bernardo Freire[a], Mihail Babcinschi[a], Lucía Ferreira[b], Baltasar Señaris[b], Felix Vidal[b], Pedro Neto[a,*]

[a]*Univ Coimbra, Centre for Mechanical Engineering, Materials and Processes, Department of Mechanical Engineering, Coimbra, Portugal*
[b]*Robotics and Control Unit, AIMEN Technology Centre, Vigo, Spain*

Abstract

Metal Additive Manufacturing (MAM) using Direct Energy Deposition (DED) is a fast-growing technological process that brings a positive boost to manufacturing industry. When compared with traditional manufacturing methods the advantages of DED are multiple, it is more cost-effective, reduces material waste and presents reduced manufacturing lead-times. However, the production of metallic parts with a complex shape is still challenging, demanding to avoid manufacturing support structures and the generation of non-horizontal and non-planar layers. Starting from the Computer-Aided Design (CAD) model of the part to produce, we propose an integrated CAD-to-part methodology featuring part decomposition, path planning, distortion and robot motion simulation, generation of the robot code and the production of the real part. Especially challenging is the path planning strategy that highly affects the final part quality. A real use case is proposed to the fabrication of an aircraft part using Laser Metal Deposition (LMD). Results demonstrate the effectiveness of the proposed methodology.

© 2020 The Authors. Published by Elsevier Ltd.
This is an open access article under the CC BY-NC-ND license (https://creativecommons.org/licenses/by-nc-nd/4.0/)
Peer-review under responsibility of the scientific committee of the FAIM 2021.

Keywords: CAD-to-part; Additive Manufacturing; Direct Energy Deposition; Complex Shape Parts

1. Introduction

Additive Manufacturing (AM) technologies, also known by 3D Printing, have gain more popularity since the late 20th century, at the time called Rapid Prototyping (RP) or Layer Manufacturing (LM) [1]. The American Society for Testing and Materials (ASTM) distinguish seven types of AM processes: binder jetting, material extrusion, material jetting, sheet lamination, vat photopolimerization, powder bed fusion and Direct Energy Deposition (DED). These standard processes can diverge in several aspects, for example feed material, need of support structures, application, cost, among others. Even so, these technologies gained the attention from different domains such as the medical sector [2] and the aerospace industry [3]. Such attention was motivated by the fact that when compared to subtractive manufacturing, AM allows to build complex parts, with less waste of material and at a competitive cost [1].

Focusing on the DED process, it generally relies on multi-axis positioners like robots or tooling machines equipped with Computer Numerical Control (CNC) controllers. These machines produce and/or repair parts in different metal alloys through melted pool methods using electric arc, electron beam or laser as heat source. Robot-based DED solutions allow to produce larger parts with high complexity level and improve the workflow of the production [4]. Besides that, robots are flexible, cheaper in relation to dedicated metal AM machines, operate in relatively large workspaces and allow on-line control and monitoring of the process. All these characteristics, which are in line with the industry 4.0 paradigm, are key for the acceptance of the technology [5].

Despite all the above advantages, it still does not exist a solution providing an integrated end-to-end approach to produce parts using DED as already exists for other AM methods, reducing both production time and the amount of human intervention. Existing studies in literature report techniques featuring the production of a small group of parts by starting from Computer-Aided Design (CAD) and ending with robot or machine code, or even methods that adapt the hardware and software from standard 3D plastic printing to print metal [6]. The necessity of avoiding support structures requires multi-axis slic-

* Corresponding author. Tel.: +351 239 790 700 ; fax: +351 239 790 701.
E-mail address: pedro.neto@dem.uc.pt (Pedro Neto).

2351-9789 © 2020 The Authors. Published by Elsevier Ltd.
This is an open access article under the CC BY-NC-ND license (https://creativecommons.org/licenses/by-nc-nd/4.0/)
Peer-review under responsibility of the scientific committee of the FAIM 2021.
10.1016/j.promfg.2020.10.094

ing processes, non-planar slices and, consequently, the use of machines with more than three degrees of freedom to produce a part, contrarily to what happens in Cartesian 3D printers [7]. In addition, metallic parts are very often expected to be fully filled with material and the tolerance for porosities is very low [8]. DED methods reach high temperature gradients, which will induce residual stress and consequently cracks and bending [8]. Furthermore, the bead geometry greatly influences the accuracy and surface finishing of the produced part [9]. These factors can be controlled by establishing an integrated AM approach considering parameters such as AM start/end points, printing direction, dwell time (wait time between layers), step over [9], velocity, intensity of the power source, among others.

The lack of CAD-to-part reliable approaches for the DED process led us to conduct this study, focusing on the definition of an integrated CAD-to-part architecture to improve the AM DED workflow. Results are supported by a real use case dedicated to the production of a complex shape part. This introductory section describes and compares the different DED techniques, AM CAD files, process and path planning, and discusses on existing techniques to implement and improve AM workflows. Section 2 enunciates the proposed integrated methodology, while the implementation on a real use case is presented in section 3. Finally, the obtained results are discussed in section 4.

1.1. Direct Energy Deposition processes

DED processes differ according to the heat source and simultaneously the feed material. The different combinations of heat source/feed material will induce different characteristics to each method. Therefore, it is possible to differentiate four individual techniques: Wire Arc Additive Manufacturing (WAAM), Laser fed with Wire (LMD-w), Electron Free Form Fabrication (EBF3) and Laser fed with Powder (LMD-p) [10].

WAAM has been considered an important AM process for the fabrication of large parts due to its high deposition rates and lower investment required [11]. This technique generates high temperature gradients, presents low accuracy and poor surface finishing, causing defects like residual stress, deformation, porosity, cracks and delamination. To avoid these issues many studies about path planning, bead modelling and process control have been conducted. LMD-w process uses a laser beam to melt the wire and generate the molten pool. The working area is involved with a shielding gas. Like in WAAM, the main concerns are centred in surface finishing, geometry and quality of the bead to achieve good microstructure and mechanical properties. The EBF3 process is similar to laser fed with wire, just diverging in the heat source that is an electron beam and in the involving environment (vacuum chamber). The EBF3 system is composed of an electron beam gun, a multi-axis position system and a metallic wire feeder [10]. LMD-p process hardware consists on a laser optics attached to a discrete coaxial powder nozzle mounted on a robotic arm or a CNC tooling machine. The melted powder solidify to form a deposited bead as the laser advances. The working area is involved with argon shielding gas. When compared to wire fed methods, LMD-p achieves better dimensional accuracy, inferior surface roughness, thinner layers and inferior deposition rates.

1.2. Process planning

Several attempts to develop a consistent CAD-to-part method can be found in the literature [7]. Although, this workflow is harder to implement as more stages are added (e.g. topology optimization, multi-physics simulation, etc.) [12], the current scenario of AM data flow involves a wide range of file types generated along the different stages of the process. This can become a problem in terms of interoperability. Each machine/robot has its own specific file format that depends on the equipment itself and the specific configuration of each working cell. Recent studies propose process planning solutions linking different stages of metal AM, including path generation, simulation and robot code generation using an AutomationML (AML) as interoperable solution [13]. Also, there was found a lack of software tools to automatically generate robot paths for complex geometries, including the path discretization process [14, 15]. In order to achieve the avoidance of support structures and material deposition in different directions by generating non-horizontal and non-planar layers, an intermediate decomposition stage is added.

1.3. Input CAD file formats

There are different CAD file formats for AM and the information that each one contains affects the efficiency of the decomposition and slicing stages of the AM process. The most common files are the Stereolithography file (STL), Additive Manufacturing File (AMF), 3D Manufacturing File (3MF) and Standard for the Exchange of Product Data file (STEP).

The STL is a standard file for AM processes, independent from the original CAD package. When compared to the original CAD file, it lacks in accuracy, affecting the final dimensional tolerance of the AM produced part. In addition, an STL file does not contain information beyond the geometry, like materials or texture [16]. The process of producing a complex part through a DED process includes a part decomposition stage to change the deposition direction and allowing the construction of overhang features [7, 17]. Owing to the lack of topological information on an STL model, it is hard to decompose a solid model regardless of the complexity and randomness of a part's geometric structure. Slicing an STL file involves a process of intercepting each facet of the file with a set of parallel planes [17]. In such a context, several studies have been conducted to test new slicing methods and ensure smaller error when creating the file [18, 16].

The AMF file format was introduced in 2009 by the ASTM committee and later defined as a standard by the International Organization for Standardization (ISO) ISO/ASTM 52915:2013. It provides support for the geometry, building material(s), colour(s), texture, constellations (representation of more than one solid in the same file) and metadata. It is technology independent, easy to implement and understand, and scalable.

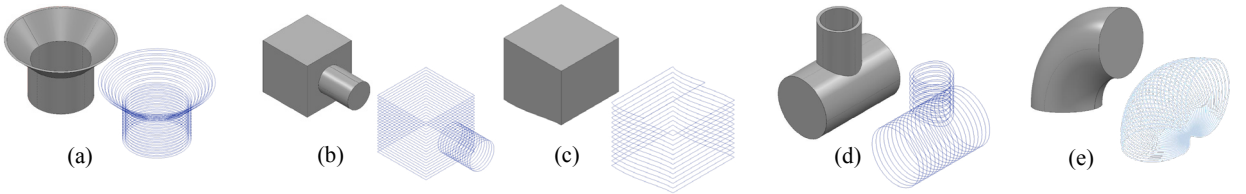

Fig. 1. Slicing methods: (a) planar and unidirectional, (b) planar and multidirectional, (c) non-planar and unidirectional, (d) non-planar and multidirectional, (e) non-parallel.

The 3MF file format represents the 3D model data for both AM and subtractive manufacturing. Such as AMF, the 3MF format is also capable of encoding the geometric data, colour, materials, texture and metadata.

The original STEP is an extensible file created to represent, archive and exchange product data during the workflow of traditional manufacturing processes. STEP is a neutral format with extensions for different applications and indutries [19]. The model represented in a STEP file can be sliced without the need of intermediate repair stages and without loss of information [20]. STEP files are more accurate than STL files [21]. Like the part decomposition stage for STL files, there are studies in the literature that describe automatic feature recognition and extraction from STEP files [23, 24]. Existing CAD packages also have its own tools capable to decompose models manually, taking advantage of Non-Uniform Rational B-Spline (NURBS) and Boundary Representation (B-Rep) based files.

1.4. Path planning: slicing and infill

Parts produced by DED are expected to be fully filled, with low porosity and free of distortion [22]. To achieve such properties, the chosen pattern and the slicing strategy have a great influence on the quality of the produced part. Depending on the part shape, numerous studies can be found in the literature describing several methods to slice the CAD model of the part. Different methodologies are categorized according to the scheme in Fig. 1. Usually, multidirectional methods require preprocessing to identify the overhang features and machines with up to 5-axis to produce them. After the slicing stage it is necessary to fill each layer contour. In literature we can find different patterns such as raster, contour offset, Medial Axis Transformation (MAT) offset, zig-zag and hybrid patterns applied to DED methods.

2. Proposed integrated methodology

The proposed CAD-to-part integrated methodology seeks to present an efficient workflow for the production of complex parts using a DED method. Our approach is summarized in Fig. 2 according to the following steps:

1. The input CAD STEP file representing the part to be produced is decomposed and a slicing direction for each feature is defined. This stage is necessary to detect different overhang features, which need different slicing directions with the purpose of avoiding support structures, or even to choose just to build a portion of the entire part;
2. Define a multi-direction non-planar slicing and generate a pattern for each layer. This stage has as inputs the bead width, layer height, the deposition strategy/pattern and a step over distance. Extract from the sliced part the AM points and the respective orientation (poses), given by the Euler angles according with the static convention. This information is extracted with respect to the original CAD frame and used to create the path file. This stage is called path generation;
3. Convert the generated path file in the Build File, the AML-based file proposed by Babcinschi et al. [13], adding to it

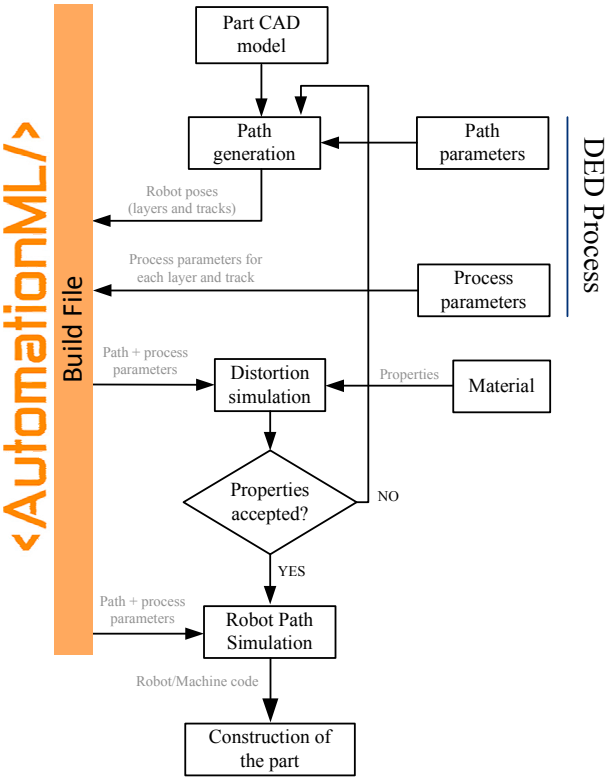

Fig. 2. Proposed approach scheme.

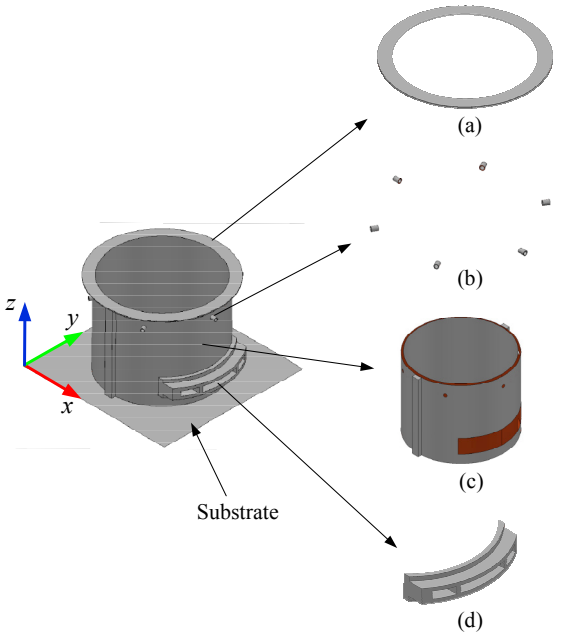

Fig. 3. Part decomposition: (a) Rim, (b) Boss x6, (c) Main body and (d) Diffuser.

the process parameters defined in previous experimental procedures;

4. Distortion simulation by reading the Build File. If the simulation result reports an unsatisfactory outcome, there is the need to re-upload the Build File and check both path and process parameters and return to the previous step. If the result is acceptable the Build File is uploaded in a robotic virtual cell previously calibrated and equal to the real one.
5. The produced paths are checked and simulated in order to avoid for example robot singularities or joint limits. The orientation of the robot tool for each point of the AM path is defined according to the Euler angles;
6. Finally, the robot code is generated and the part is produced using a DED technology.

3. Implementation

We selected an aircraft component to be our case study part, Fig. 3. It presents a relatively challenging geometry, being ideal to test our proposed CAD-to-part methodology.

3.1. Part decomposition and slicing direction

The CAD part was decomposed in a total of nine features, Fig. 3, namely the (1) Main body, (2) Diffuser, (3) Rim and (4) six Bosses. This stage was achieved by using off-the-shelf tools in CAD packages that allow to segregate different surfaces of a STEP model. This process is accomplished by taking advantage

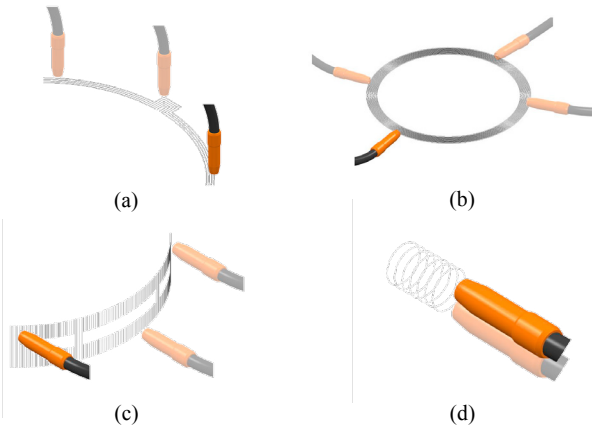

Fig. 4. Patterns for the different features with representation of the respective tool orientation: (a) Main Body (contour offset), (b) Rim (raster), (c) Diffuser (raster), (d) Bosses (MAT offset).

of the B-Rep used in STEP file format and gives to the user a total control of the decomposition process.

The slicing direction of each feature was chosen in order to guarantee the existence of a base during the deposition process, as summarized in Table 1.

Table 1. Slicing direction for each part feature. **An increment of 60° around Z for each one of the other bosses.

Feature	Slicing direction
Main body	Z+
Diffuser	X+
Rim	X+ (radial)
Bosses (x6)	X+ for the first boss **

3.2. Slicing and path planning

The path parameters that achieved the ideal bead geometry were obtained by previous experimental tests:

- Bead width: 2.15 mm;
- Step over: 1.2 mm;
- Layer height: 0.73 mm.

We used different infill patterns for each feature. For the Main body it was used a perimeter offset with a coaxial tool orientation, Fig. 4 (a). For the Diffuser and the Rim it was used a raster pattern. A fixed tool orientation was defined for the Diffuser and a dynamic tool orientation for the Rim, Fig. 4 (c) and Fig. 4 (b), respectively. Finally, for each Boss the chosen pattern was MAT offset with fixed tool orientation, Fig. 4 (d).

3.3. Conversion of the generated path in a Build File

Using our software to generate the AML-based data file for linking the different stages of metal AM process, [13], the file

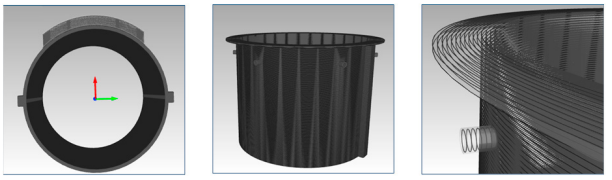

Fig. 5. Visualization of part paths from the Build File.

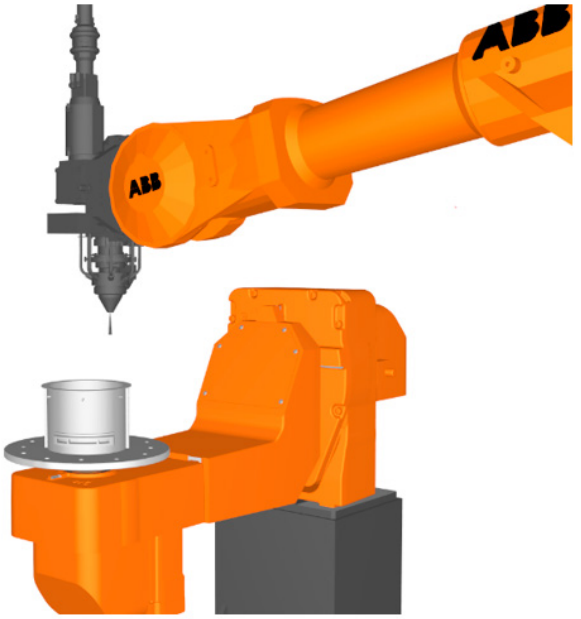

Fig. 6. Simulation environment of the robotic cell.

structure divides the process parameters as track and layer parameters. For the LMD-p case the track process parameters are laser power, velocity and shielding gas flow, while the layer parameters are dwell time, powder feed rate, travel velocity, and spot diameter. Despite the possibility to vary parameters along the process, these were kept as constant during the whole manufacturing of the part. Through previous experiments these process parameters were adjusted to perform the referred path parameters (bead width, step over and layer height).

3.4. Distortion simulation

The distortion simulation begins by reading the AML Build File containing the required part points and parameters. This stage allows to identify the most critical areas during the manufacturing process that will be the source of possible defects. It is also possible to iterate on the different parameters of the manufacturing strategy virtually and thus determine the optimal parameters.

The analysis of the distortions generated in the part after the manufacturing process also allows to obtain the counter-deformed geometry that compensates for the distortions generated during the additive manufacturing process, and giving as

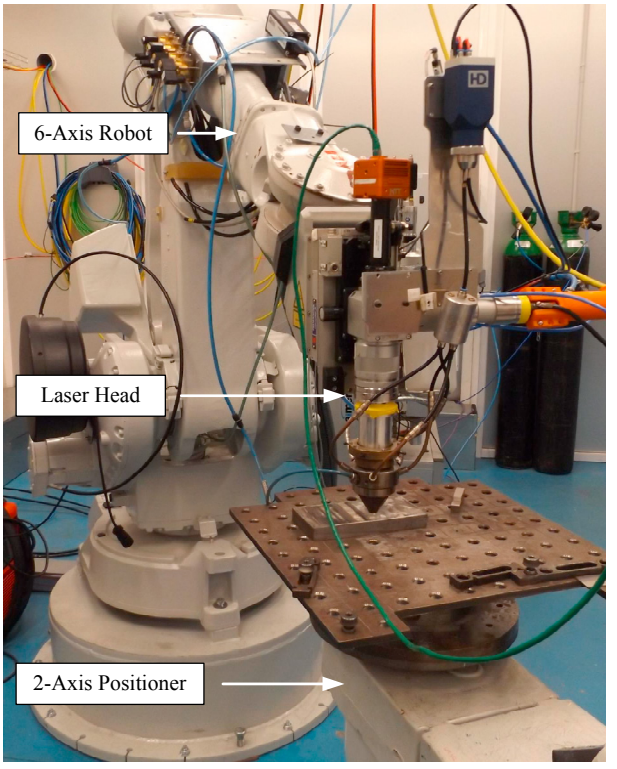

Fig. 7. Robotic cell layout.

the final result the objective geometry within the established tolerance.

3.5. Path simulation

According to the feedback from the simulation stage the Build File graphical user interface (GUI) software allows to update the process parameters of each specific track or layer, as well as to visualize such paths, Fig. 5.

After adjusting the process parameters, all the points were imported to a virtual robotic cell representing the real one. The reachability of each point was tested in the virtual/simulation environment and the robot code was generated, Fig. 6.

3.6. Production

The robotic cell layout is composed by a 6-axis ABB IRB 4400/60 and a 2-axis positioner ABB IRBP A250 where the base of the part is fixed. The cladding head is a Trumpf BEO D70, the nozzle a Fraunhofer IWS model, the coaxial monitoring system is from Clamir, the laser system is a Trumpf TruDisk 16002 and the powder feeder is a Medicoat DUO, Fig. 7.

The rotation of the 2-axis positioner allows to rotate the part during the production, Fig. 8, in order to keep the laser head coaxial and achieve the desired orientation for each feature, Fig. 4. The part was produced in stainless steel 316L using LMD-p process and the argon as protection gas.

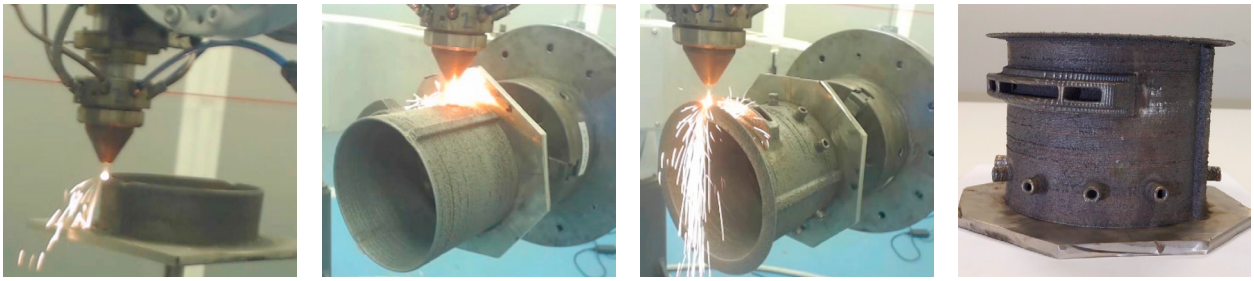

Fig. 8. Sequence of the production of the target part.

Table 2. Features and associated patterns.

	Main body	Diffuser	Rim	Boss	Main body	Diffuser
Strategy	Outer line offset	Raster (0°)	Raster	MAT offset	MAT offset	Raster (90°)
Points	39303	6412	2026	119	91210	4802
Tracks	724	3206	24	7	2169	636
Layers	121	16	12	7	121	16
AML file size	37.30 MB	9.67 MB	1.96 MB	140 KB	87.50 MB	5.30 MB

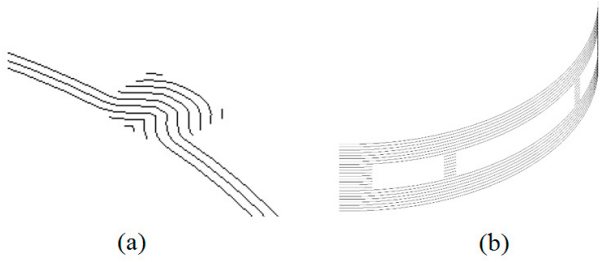

Fig. 9. (a) Main Body MAT offset pattern and (b) Diffuser with Raster (90°) pattern.

4. Results and discussion

Using the proposed methodology, the target part was successfully produced, and the interoperability between the different stages of the process (decomposition, slicing, path planning, simulation and robot simulation) was successfully achieved.

The usage of a STEP file had a positive impact on the workflow by giving to the user the possibility of total control in the part decomposition stage. It is time consuming for the user but less computational expensive when compared to the reported studies in literature in which only a small set of pieces fits [7, 17].

Table 2 summarizes the number of points, tracks, layers and the AML file size obtained for the different paths used in each feature. It also presents the comparison for the production of the Main body and Diffuser features using different paths, the MAT based offset and the 90° rotated raster, Fig. 9. These strategies demonstrated to be equally feasible. Since Rim and the Boss features are cylindrical parts, the strategies we studied rely on circular patterns. It is also visible that changing the outer line offset to MAT offset increases the number of points of the path in the case of Main body. In addition, using MAT offset generates a heavier file, increasing the computational effort and turning the process more time consuming in the downstream stages.

5. Conclusion

In this study we presented an integrated metal additive manufacturing CAD-to-part methodology featuring part decomposition, path planning, simulation of robot motion, generation of the robot code and the production of the real part. Different path patterns were studied and associated to different part features after the decomposition of a more complex part. Interoperability of systems using AML was also successfully implemented. Results from a real use case dedicated to the fabrication of an aircraft part using LMD-p demonstrate the effectiveness of the proposed methodology.

Acknowledgements

This research was partially supported by European Union's Horizon 2020 under grant agreement No 820776 (project integradde), Portugal 2020 project DM4Manufacturing POCI-01-0145-FEDER-016418 by UE/FEDER through the program COMPETE 2020, and the Fundação para a Ciência e a Tecnologia COBOTIS project (PTDC/EME-EME/32595/2017). This research is also sponsored by FEDER funds through the program COMPETE Programa Operacional Factores de Competitividade, and by national funds through FCT Fundação para a Ciência e a Tecnologia under the project UIDB/00285/2020.

References

[1] Wong, K. V., Hernandez, A., 2012. A Review of Additive Manufacturing. International scholarly research notices 2012, 1–10.

[2] Javaid, M., Haleem, A., 2017. Additive manufacturing applications in medical cases: A literature based review. Alexandria Journal of Medicine 54.4, 411–422.
[3] Seabra, M., Azevedo, J., Arajo, A., Reis, L., Pinto, E., Alves, N., Santos, R., Mortgua, J. P., 2016. Selective laser melting (SLM) and topology optimization for lighter aerospace components. Procedia Structural Integrity 1, 289–296.
[4] Barnett, E., Grosselin, C., 2015. Large-scale 3D printing with a cable-suspended robot. Additive Manufacturing 7, 27–44.
[5] Ding, Y., Warton, J., Kovacevic, R., 2016. Development of sensing and control system for robotized laser-based direct metal addition system. Additive Manufacturing 10, 24–35.
[6] Nilsiam, Y., Sanders, P., Pearce, J. M., 2017. Slicer and process improvements for open-source GMAW-based metal 3-D printing. Additive Manufacturing 18, 110–120.
[7] Ding, Y., Dwivedi, R., Kovacevic, R., 2017. Process planning for 8-axis robotized laser-based direct metal deposition system: A case on building revolved part. Robotics and Computer-Integrated Manufacturing 44, 67–76.
[8] Liu, S., Shin, Y. C., 2019. Additive manufacturing of Ti6Al4V alloy: A review. Materials and Design 164, 107552.
[9] Ding, D., Pan, Z., Cuiuri, D., Li, H., 2015. A multi-bead overlapping model for robotic wire and arc additive manufacturing (WAAM). Robotics and Computer-Integrated Manufacturing 31, 101–110.
[10] Ding, D., Pan, Z., Cuiuri, D., Li, H., 2015. Wire-feed additive manufacturing of metal components: technologies, developments and future interests. The International Journal of Advanced Manufacturing Technology 81, 465–481.
[11] Tabernero, I., Paskual, A., lvarez, P., Surez, A., 2018. Study on Arc Welding Processes for High Deposition Rate Additive Manufacturing. Procedia CIRP 68, 358–362.
[12] Francois, M. M., Sun, A., King, W. E., Henson, N. J., Tourret, D., Bronkhorst, C. A., Carson, N. N., Newman, C. K., Haut, T., Bakosi, J., Gibbs, J. W., Livescu, V., Vander Wiel, S. A., Clark, A. J., Schraad, M. W., Blacker, T., Lim, H., Rodgers, T., Owen, S., Abdeljawad, F., Madison, J., Anderson, A. T., Fattebert, J-L., Ferencz, R. M., Hodge, N. E., Khairallah, S. A., Walton, O., 2017. Modeling of additive manufacturing processes for metals: Challenges and opportunities. Current Opinion in Solid State and Materials Science 21, 198–206.
[13] Babcinschi, M., Freire, B., Neto, P., Ferreira, L. A., Searis, B. L., Vidal, F., 2019. AutomationML for Data Exchange in the Robotic Process of Metal Additive Manufacturing. 24th IEEE International Conference on Emerging Technologies and Factory Automation (ETFA). IEEE 2019, 65–70.
[14] Mendes, N., Neto, P., Pires, N., Loureiro, A., 2013. Discretization and fitting of nominal data for autonomous robots. Expert Systems with Applications 40.4, 1143–1151.
[15] Ferreira, M., Moreira, A.P., Neto, P., 2012. A low-cost laser scanning solution for flexible robotic cells: spray coating. The International Journal of Advanced Manufacturing Technology 58, 1031–1041.
[16] Huang, S. H., Zhang, L. C., Han, M., 2002. An effective error-tolerance slicing algorithm for STL files. The international Journal of Advanced Manufacturing Technology 20.5, 363–367.
[17] Ding, D., Pan, Z., Cuiuri, D., Li, H., Larkin, N., Van Duin, S., 2016. Automatic multi-direction slicing algorithms for wire based additive manufacturing. Robotics and Computer-Integrated Manufacturing 37, 139–150.
[18] Zha, W., Anand, S., 2015. Geometric approaches to input file modification for part quality improvement in additive manufacturing. Journal of Manufacturing Processes 20, 465–477.
[19] Qin, Y., Qi, Q., Scott, P. J., Jiang, X., 2019. Status, comparison, and future of the representation of additive manufacturing data. Computer-Aided Design 111, 44–64.
[20] Starly, B., Lau, A., Sun, W., Lau, W., Bradbury, T., 2005. Direct slicing of STEP based NURBS models for layered manufacturing. Computer-Aided Design 37.4, 387–397.
[21] Bijnens, J., Kellens, Cheshire, D., 2018. Accuracy of geometry data exchange using STEP AP242. Procedia CIRP 78, 219–224.
[22] Ren, K., Chew, Y., Fuh, J. Y. H., Zhang, Y. F., Bi, G. J., 2019. Thermo-mechanical analyses for optimized path planning in laser aided additive manufacturing processes. Materials and Design, 162, 80–93.
[23] Kim, B.C., Mun, D., 2014. Feature-Based simplification of boundary representation models using sequential iterative volume decomposition, Computers and Graphics, 38.1, 97–107.
[24] Woo, Y., Sakurai, H., 2002. Recognition of maximal features by volume decomposition, Computer Aided Design, 34.3, 195–207.